Xu *et al. AAPS Open* (2023) 9:16
https://doi.org/10.1186/s41120-023-00083-8

AAPS Open

RESEARCH Open Access

Preparation, characterization, and biological activity of the inclusion complex of dihydroquercetin and β-Cyclodextrin

Yaping Xu[1], Yue Wang[2], Chujie Li[2], Tao Han[1], Haiming Chen[1,3], Wenxue Chen[1], Qiuping Zhong[1], Jianfei Pei[1], Guido R. M. M. Haenen[2], Zhengwen Li[4], Mohamed Moalin[5], Ming Zhang[1*] and Weijun Chen[1*]

Abstract

Dihydroquercetin (DHQ) is a natural occurring dihydroflavonol that has strong antioxidant and antibacterial activities. However, its application is limited due to its poor solubility. This study aims to improve the aqueous solubility of DHQ by complexing DHQ with β-cyclodextrin (β-CD) to boost its biological activity. DHQ was encapsulated with β-CD by freeze drying at a 1:1-M ratio. The structure of DHQ/β-CD complex prepared was elucidated by using Fourier transform infrared spectroscopy, differential scanning calorimetry, X-ray diffraction, scanning electron microscopy, and ^{1}H nuclear magnetic resonance (^{1}H NMR). In addition, molecular docking further revealed two energetically favorable conformations of the DHQ/β-CD complex, in which DHQ interacted with β-CD via hydrogen bonds. Experimental results showed that the solubility of the DHQ increased 22.63-fold by encapsulating with β-CD. Also the dissolution rate, antioxidant activity and antibacterial activity of the DHQ were significantly improved by encapsulating. The encapsulating with β-CD solves the problem of the poor aqueous solubility of DHQ, and broadens the path for a more optimal use of the health promoting effect of DHQ in pharmaceutical and food products.

Keywords Dihydroquercetin, β-cyclodextrin, Complex, Encapsulation, Solubility

Introduction

Dihydroquercetin (DHQ), also known as taxfolin, is a dihydroflavonol commonly found in Pseudotsuga taxifolia (Yan et al. 2017). DHQ has been in the spotlight because of its potent antioxidant activity (Kurth and Frank 1951), which is linked to its antitumor, anti-inflammatory, anti-proliferative, anti-diabetic, anti-microbial, anti-platelet aggregation and antiviral activity (Wen et al. 2017; Lia et al. 2016). Moreover, DHQ is also used as supplement to improve health and as additive to extend the shelf life of some food products, like chocolate, milk powder, and other fat rich products. However, valorizing the potential of DHQ is restricted by its poor water solubility.

Several strategies have been used to improve the water solubility of DHQ, such as nanodispersion (Yuangang et al. 2014), crystal engineering (Selivanova and Terekhov 2020), and chemical modification (Lia et al. 2016). An emerging technology, which has gained great and

*Correspondence:
Ming Zhang
m.zhang@hainanu.edu.cn
Weijun Chen
chenwj@hainanu.edu.cn
[1] College of Food Science and Engineering, Hainan University, 58 Renmin Road, Haikou 570228, Hainan, China
[2] Department of Pharmacology and Personalized Medicine, School of Nutrition and Translational Research in Metabolism (NUTRIM); Cardiovascular Research Institute= Maastricht (CARIM), Faculty of Health, Medicine and Life Sciences, Maastricht University, Maastricht, MD 6200, the Netherlands
[3] Maritime Academy, Hainan Vocational University of Science and Technology, 18 Qiongshan Road, Haikou 571126, PR China
[4] School of Pharmacy, Chengdu University, 2025 Chengluo Avenue, Chengdu 610106, Sichuan, China
[5] Research Centre Material Sciences, Zuyd University of Applied Science, 6400 AN Heerlen, the Netherlands

increasing interest in improving the solubility of hydrophobic compounds is encapsulation by Cyclodextrins (CDs) (Priya and Meenakshi 2020). CDs, which can be obtained from the enzymatic degradation of linear starch (Qi and Zimmermann 2005), are a class of cyclic oligosaccharides consisting of 6, 7, and 8 D-glucopyranose units linked by α-D-(1,4) bonds in a cyclic manner and named α-, β-, and γ-CD respectively (Song and William 1992). CDs have a toroidal, donut-like shape, in which the inner cavity is hydrophobic due to the oxygen and hydrogen atoms in the glycosidic bond and the outside is hydrophilic because of exposed free hydroxyl groups (Conceicao et al. 2018; Crini 2014). The unique structure enables CDs to form inclusion complexes with various hydrophobic guest molecules by van der Waals forces and hydrogen bonds to increase the solubility of bioactive compounds (Priya and Meenakshi 2020) (Fig. 1). Among the natural CDs, β-CD has been more broadly studied and applied in pharmaceutical and food industry than α-CD and γ-CD because of its moderate cavity size, ease of preparation, relatively low cost and its capability to improve the physical, chemical, and biological properties of bioactive molecules (Liu et al. 2020). For example, Farahat et al. prepared clove essential oil/β-CD complex to improve the antibacterial activity against a variety of bacteria (Farahat 2020), and Imiquimod/β-CD complex prepared by Guedes et al. greatly improved the solubility of Imiquimod to develop pharmaceuticals in aqueous solution (Guedes et al. 2020).

This study aims to improve the aqueous solubility of DHQ by complexing with β-CD and to boost its biological activity. It is different from the preparation method of previous study (Yang et al. 2011). The DHQ/β-CD complex was prepared by freeze drying. The structure and properties of the inclusion complex were studied by using ultraviolet spectroscopy (UV), Fourier transform infrared spectroscopy (FTIR), differential scanning (DSC), X-ray diffraction (XRD), scanning electron microscopy (SEM) and ^{1}H nuclear magnetic resonance (^{1}H NMR). Molecular docking calculation was used to find the energetically most favorable conformations of DHQ/β-CD complex at the molecular level. The effects of the encapsulation on DHQ's solubility, dissolution rate, thermal stability, antioxidant activity and antibacterial activity were determined. Studying the encapsulation by β-CD provides a theoretical support to solve the poor aqueous solubility of DHQ, and to promote its application in the pharmaceutical and food industries.

Materials and methods

Materials

DHQ (FW = 304.25, purity ≥ 99%) was obtained from Maclean Biochemical Technology Co., Ltd. (Shanghai, China). β-CD (FW = 1134.98, purity ≥ 98%) was acquired from Hynes Optech Co., Ltd. (Tian Jing, China). Anhydrous ethanol was provided by Sinopharm Chemical Reagent Co, Ltd. (Shanghai, China). Other reagents and chemicals were of analytical grade and used without

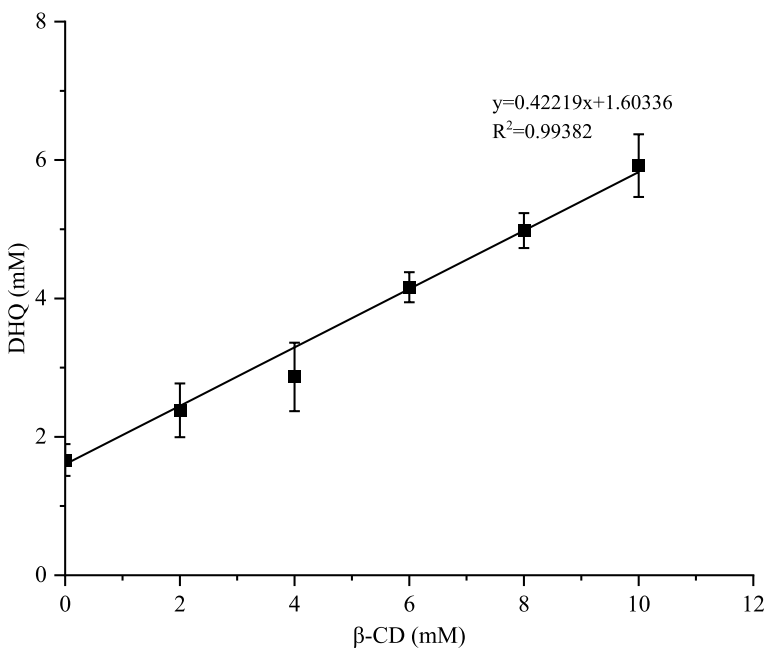

Fig. 1 Phase solubility diagram of DHQ in the aqueous solution of β-CD at 30 ℃. The apparent solubility of the DHQ (Y-axis) linearly increases with the concentration of β-CD (X-axis) according to the equation given in the figure

further purification. Ultra-pure water was used throughout the experiment.

Phase solubility study

DHQ (0.006 g) was slowly added to 10 mL β-CD working solution with concentrations of 2, 4, 6, 8, and 10 mM, respectively. The reaction mixture was shaken at 150 rpm in a water bath at 30 °C for 24 h in dark to achieve dynamic equilibrium. The samples were filtered over a 0.22 μm filter and the absorption at 290 nm (A_{290}) was determined using a UV–Vis spectrophotometer UV-5500P (Yuananalysis Instruments Co., Ltd., Shanghai, China). 3.04 mg of DHQ powder was dissolved in 10 mL water to make 1 mmol/L aqueous solution, which was then diluted by water into 0.02 mM, 0.04 mM, 0.06 mM, 0.08 mM, and 0.1 mM DHQ standard solutions, respectively. The content of DHQ can be calibrated by the following equation from the standard curve: $A_{290} = 8.3544\ C + 0.0319$ ($R^2 = 0.997$). The concentration of DHQ (on the *Y*-axis) was plotted against the concentration of β-CD (*X*-axis), to obtain the phase solubility curve (Zhou et al. 2022). The apparent stability constant ($K_{1:1}$) of inclusion complex was calculated based on the phase solubility diagram according to the Higuchi-Connors Eq. (1).

$$K = \frac{\text{Slope}}{S_0(1 - \text{Slope})} \quad (1)$$

where *K* is the apparent stability constant (M^{-1}), S_0 is the solubility of DHQ in the absence of β-CD at 30 °C and the Slope is obtained from a linear regression of the data points of the plot.

Preparation of complex

The DHQ/β-CD complex was prepared by freeze drying. The mixture of DHQ and β-CD (0.14 g) in a 1:1-M ratio was dissolved in 50 mL of ethanol/water (3/2, v/v) solution. The mixture of DHQ and β-CD was stirred at 150 rpm in the water bath at 30 °C for 4 h in dark followed by centrifugation of the suspension at 12,000 rpm and 4 °C for 10 min. The obtained supernatant was filtered through 0.22 μm filter, after which ethanol was evaporated by Rotary evaporator SENCO (Shensheng Technology Co., Ltd., Huizhou, China) at 60 °C and 110 rpm for 10 min. The obtained solution was frozen overnight in a refrigerator at − 80 °C and then subjected to the freeze-drier SCIENTZ-10N (Xinzhi Biological Technology Co., Ltd., Ningbo, China) for 48 h to obtain the final product in the form of a light yellow solid powder, which was the DHQ/β-CD complex (Carlotti et al. 2011; Savic et al. 2015).

Preparation of physical mixture

The physical mixture was prepared by weighing and mixing DHQ and β-CD in a 1:1-M ratio and thoroughly grinding (Benguo et al. 2013).

FTIR

DHQ, β-CD, DHQ/β-CD physical mixture and DHQ/β-CD complex were separately mixed and pressed with KBr in a ratio of 1:30, and KBr alone was used as blank control. Then the FTIR spectra were recorded in the wavenumber range of 4000–400 cm^{-1} using FTIR spectrometer T27 (BRUKER Company, Germany) (Qian et al. 2018).

DSC

Thermal analysis of DHQ, β-CD, DHQ/β-CD physical mixture and DHQ/β-CD complex was performed by a synchronous thermal analyzer DSC131EVO (Xinghe instruments Co., Ltd., Shanghai, China). For DSC measurements, the gas flow rate was 20 mL/min and the temperature range was 30 ~ 350 °C, with the scanning rate of 16 K/min (Kim 2020).

XRD

The XRD patterns of DHQ, β-CD, DHQ/β-CD physical mixture and DHQ/β-CD complex was analyzed using X-ray diffractometer DX-2700BH (Haoyuan Instruments Co., Ltd., Dandong, China). The voltage and the strength of the electric current were 40 kV and 40 mA, respectively. The diffraction angle ranged from 10° to 60°. The crystallinity was derived from the software MDI Jade 6 (Materials Data, CA, USA) (Viswalingam et al. 2016).

^{1}H NMR

^{1}H NMR spectra of β-CD and DHQ/β-CD complex were recorded by a NMR spectrometer Advance 400 (Bruker, USA), with the operating frequency of 400 MHz, in a 5-mm diameter glass cuvette at room temperature (Silva et al. 2020). D_2O was used as the solvent.

Molecular docking

Autodock tools-1.5.6 (The Olson Laboratory, Scripps Research Institute, CA, USA) was used for molecular docking. The structure of DHQ and β-CD were downloaded through PubChem organic small molecule bioactivity database. The molecule structure of β-CD and DHQ were optimized to minimize the energy of the 3D structure by ChemDraw 18.0 and Chem3D 18.0 (CambridgeSoft, MA, USA). The receptor remained rigid, and the ligand remained flexible. The autogrid

box parameter was set at 80 Å × 80 Å × 100 Å, and the grid spacing parameter was 0.375 Å. The calculation was performed using the Lamarckian genetic algorithm (LGA), and other parameters were set to default values. The DHQ molecule could move over the whole region of the β-CD with 100 runs to obtain all the possible binding positions. Pymol 2.2 (Schrödinger Inc., NY, USA) was used to analyze docking results (He et al. 2022).

SEM

The surface morphology of DHQ, β-CD, DHQ/β-CD physical mixture, and DHQ/β-CD complex was analyzed by SEM S-3000N (Hitachi, Ltd., Tokyo, Japan) under the acceleration of 5 kV. Before determination, samples were placed on a sample table affixed with carbon conductive tape, spread evenly and placed under a certain vacuum for ion sputtering gold plating. Photomicrographs were taken at magnification factor for × 2000 (Liu et al. 2022).

Particle size, solubility, and dissolution rate

Sample suspensions were prepared by dissolving DHQ and DHQ/β-CD complex separately in 10 mL ultrapure water at 25 ± 1 °C. The particle size was determined in triplicate using a Laser Particle Size Analyzer MAL1077738 (Spectrum Instrument Systems, Shanghai, China) (Cenobio-Galindo et al. 2019).

An excess amount of DHQ and DHQ/β-CD complex were added to 1000 mL of ultrapure water and oscillated at 25 ± 1 °C for 24, 30, and 36 h, respectively, to achieve a steady state. After centrifuging at 12,000 r/min for 10 min, the supernatant was passed through a 0.22-μm aqueous filter and determined by UV spectrophotometer mentioned above. The solubility was obtained according to the standard curve (Huo et al. 2020).

The dissolution rate of DHQ and DHQ/β-CD complex in phosphate buffer (PBS, PH = 7.4, 0.1 M) was studied on the premise of maintaining the sink condition and detected by UV spectrophotometer. The speed and the dissolution temperature were 50 r/min and 37 ± 1 °C, respectively. Samples were taken by syringe within 30 s at different intervals (0, 5, 10, 20, 40, 80, 160, 320, 480, 640, 800 min). The sum of the volumes for collected samples should be within 1% of original samples. The solutions were centrifuged at 12,000 r/min for 10 min, and diluted 100 times after passing through a 0.22-μm filter and then measured by UV spectrophotometer. The concentrations were derived from the standard curve, and the dissolution rates were obtained (Yuangang et al. 2014; Wan et al. 2021).

TGA

The weight loss of DHQ and DHQ/β-CD complex was determined with a Thermogravimetric analyzer Q600 (TA INSTRUMENTS, USA). Five milligrams of DHQ and DHQ/β-CD complex was uniformly spread in the crucible and heated in a dynamic nitrogen atmosphere from 30 °C to 600 °C, with a heating rate of 10 °C/min and flow rate of 20 mL/min (Katanic et al. 2015).

Antioxidant activity

Determination of DPPH radical scavenging activity

The 1,1-diphenyl-2-picrylhydrazyl (DPPH) radical scavenging activity of DHQ and DHQ/β-CD complex was measured by the method of Li et al., with slight modifications (Lia et al. 2016). Twenty microliters of DHQ (0.01 ~ 0.06 mM) was added to 380 uL of DPPH solution, and the mixture was shaken energetically and placed at room temperature in dark for 20 min. The same procedure was performed for DHQ/β-CD complex. Subsequently, 200 μL of the incubation mixture was taken to a 96-well plate to determine the absorbance value at 515 nm using a Microplate Reader Synergy LX (BIOTEK INSTRUMENTS, INC, USA), with acetic acid buffer (pH = 5, 0.01 M) as the blank control. The DPPH radical scavenging activity was calculated according to Eq. (2):

$$\mathrm{DPPH}\ (\%) = (\mathrm{A}_0 - \mathrm{A}_1)/\mathrm{A}_0 \times 100\% \tag{2}$$

where A_0 is the absorbance of blank control, A_1 is the absorbance of the sample in reactive system.

Determination of ABTS radical scavenging activity

The 2,2 ’-azinobis-3-ethylbenzothiazoline-6-sulphonic acid (ABTS) radical scavenging activity of DHQ and DHQ/β-CD complex was evaluated by the method of El-Hadad et al. (Cao et al. 2012), with slight modifications. Ten microliters of each sample at different DHQ concentrations (0.005 ~ 0.01 mM) was added to 190 μL of ABTS solution. The same procedure was performed for DHQ/β-CD complex. Samples were taken to a 96-well plate to determine the reduction in absorbance at 734 nm using a Microplate Reader in 10 min. PBS was used as the blank control. The ABTS radical scavenging activity was calculated according to Eq. (3):

$$\mathrm{ABTS}\ (\%) = (\mathrm{A}_0 - \mathrm{A}_1)/\mathrm{A}_0 \times 100\% \tag{3}$$

where A_0 is the absorbance of blank control, A_1 is the absorbance of the sample in reactive system.

Antibacterial activity

The bacterial strains of *E. coli* BNCC133264 was inoculated into 60 mL of sterile nutrient broth and incubated at 37 °C for 24 h. The sterile pipette was used to transfer 500 μL bacterial suspensions to spread evenly on a plate

which was poured with complete medium (Shanmugam et al. 2016). The DHQ and DHQ/β-CD complex solutions that contained equal concentrations of DHQ were prepared to obtain the samples with concentrations of 0.4, 0.8, 1.2, 1.6, and 2.0 mg/mL. Filter papers with a diameter of 0.6 cm were used as some experimental diffusion discs (Wang et al. 2011). The filter paper was soaked in the sample to be tested, and then the test plate was put in the incubator. After 24 h, the diameter of the inhibition circle was measured using vernier calipers. The average size of the diameters was determined for each condition for three measurements (Zhang et al. 2020).

Statistical analysis

All experiments were performed at least in triplicate. Data were given as mean ± standard error of the mean (S.E.M.) or as a typical example.

Results and discussion

Phase solubility study

The analysis of phase solubility was carried out to determine the solubility and complexing ability of DHQ with β-CD. The phase solubility diagram of DHQ in β-CD at 30 °C is shown in Fig. 1. The apparent stability constant, K had a value of 455.7 M^{-1}. When the K value is between 50 and 5000 M^{-1}, the host molecule is effective in increasing the solubility of a hydrophobic guest molecule, and the inclusion complex formed tends to have a good stability (Sadaquat and Akhtar 2020). The apparent solubility of the DHQ appeared to increase linearly with concentration of β-CD (Fig. 1). This indicates that the inclusion ratio of DHQ and β-CD was 1:1 (Brewster and Loftsson 2007). When the concentration of β-CD was 10 mM, the solubility of DHQ increased to 5.91 ± 0.45 mM, which was 3.56 times higher than the solubility of DHQ without β-CD (1.66 ± 0.23 mM).

FTIR analysis

FTIR absorption was applied to assign the functional groups, which form the interaction between β-CD as the host molecule and DHQ as the guest molecule. The FTIR spectra are depicted in Fig. 2A. In the FTIR spectrum of β-CD, the characteristic absorption peaks located at 3433 cm^{-1}, 2924 cm^{-1}, and 1028 cm^{-1} represents the stretching of –OH bond, –C–H bond and –C–O bond, respectively (Khanna and Chakraborty 2018). And the absorption band occurring at 1159 cm^{-1} was caused by asymmetric stretching vibrations of the C–O–C glycosidic bridge (Silva et al. 2020). In the FTIR spectrum of DHQ, the characteristic absorption band at 3410 cm^{-1} was caused by the vibration of the –OH. The broad 1639 cm^{-1} band in the crystalline DHQ spectrum is mainly contributed from the C=O stretching and OH bending and the 1460 cm^{-1} band is likely associated with C–H bending (Zu et al. 2014; Khlupova et al. 2016). The absorption bands at 1276 cm^{-1} and 1367 cm^{-1} were assigned to the vibration of C=O and C–O–C, respectively (Yuangang et al. 2014). As shown in Fig. 2A, the FTIR spectrum of DHQ/β-CD physical mixture showed the overlap of FTIR diagrams of DHQ and β-CD, indicating that DHQ has not been encapsulated into β-CD. The FTIR spectrum of DHQ/β-CD complex was significantly different from that of DHQ and β-CD. The absorption bands intensities for DHQ at 1276 cm^{-1} (C=O), 1367 cm^{-1} (C–O–C) and 1460 cm^{-1} (C–H) were greatly reduced in the FTIR spectrum of DHQ/β-CD complex. Apparently in the inclusion complex, when DHQ is in the cavity of β-CD, the vibrations of the groups are restricted. In the FTIR spectrum of β-CD, there is a higher absorption intensity at 1159 cm^{-1} and 1028 cm^{-1}. However, in the DHQ/β-CD complex, the intensity of the corresponding absorption band decreases and slightly shifts. These indicated the existence of interactions between DHQ and β-CD. No new absorption peaks were observed in the FTIR spectrum of DHQ/β-CD complex, comparing with that of DHQ and β-CD. It confirms that no new covalent bonds are formed during complexing.

DSC analysis

DSC was used to further study the formation of the complex between DHQ and β-CD. The DSC results of DHQ, β-CD, DHQ/β-CD physical mixture, and DHQ/β-CD complex are shown in Fig. 2B. The DSC curve of the DHQ exhibited an endothermic peak at 247 °C, corresponding to its melting points. While β-CD showed endothermic peaks at 153 °C and 316 °C, which correspond to the loss of bound water and self-decomposition, respectively. The DSC curve of the DHQ/β-CD physical mixture was similar to that of β-CD, which indicates that when β-CD and DHQ were simply mixed, no new phase was generated. However, there was almost no endothermic peak in the DSC curve of the DHQ/β-CD complex, which differed a lot from that of the DHQ/β-CD physical mixture. Probably, the water that was present in the cavity of β-CD has been exchanged for DHQ in the inclusion complex, which can explain the disappearance of absorption peaks at 153 °C.

XRD analysis

The change of the material crystal before and after complexing was analyzed by XRD. X-rays will be diffracted as they pass through the crystal, which can provide an indirect evidence for the complex formation. As shown in Fig. 2C, the XRD pattern of DHQ was in the typical crystalline state, which presented numerous well-defined and intense diffraction peaks: 14.14° (94.17%), 18.76°

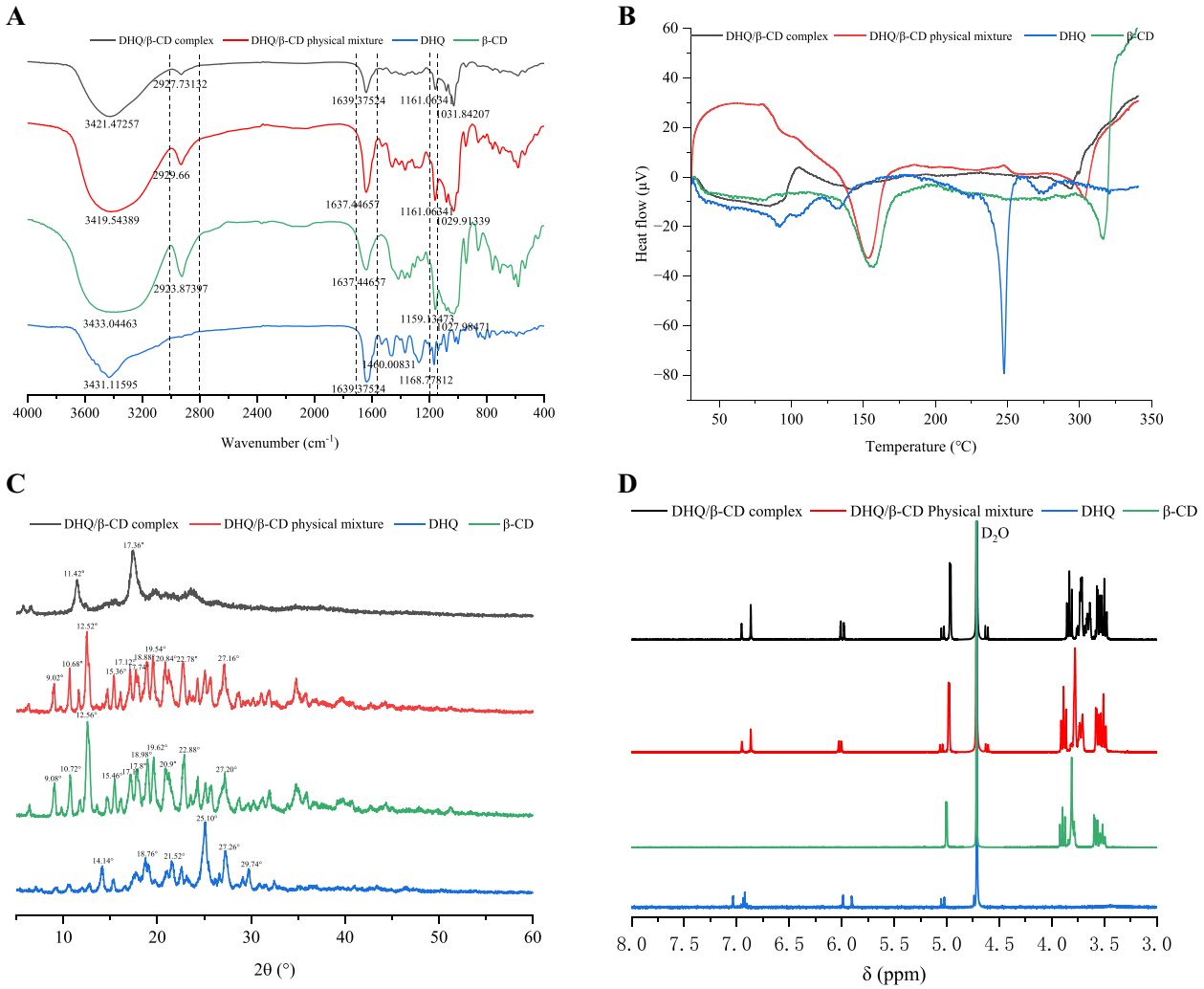

Fig. 2 **A** is the FTIR spectra of DHQ, β-CD, DHQ/β-CD physical mixture, and DHQ/β-CD complex. **B** is the DSC curves of DHQ, β-CD, DHQ/β-CD physical mixture, and DHQ/β-CD complex. **C** is the XRD patterns of DHQ, β-CD, DHQ/β-CD physical mixture, and DHQ/β-CD complex. **D** is the ^{1}H NMR spectra of DHQ, β-CD, DHQ/β-CD physical mixture, and DHQ/β-CD complex

(81.68%), 21.52° (89.34%), 25.1° (68.41%), 27.26° (82.73%), and 29.74° (99.9%). This diffraction pattern was consistent to previous report (Yuangang et al. 2014). The XRD pattern of β-CD was also in the typical crystalline state, in which diffraction peaks were 9.08° (98.08%), 10.72° (97.13%), 12.56° (91.78%), 15.46° (97.33%), 17.1° (96.69%), 17.8° (94.38%), 18.98° (95.00%), 19.62° (94.81%), 20.9° (95.79%), 22.88° (94.51%), and 27.20° (96.22%). The XRD pattern of the DHQ/β-CD physical mixture was the superposition of the XRD patterns of the DHQ and β-CD, which indicates that the crystal form of the DHQ and β-CD were not changed when they were physically mixed. However, the XRD pattern of the DHQ/β-CD complex was totally different from that of the DHQ/β-CD physical mixture. It is worth noting that the sharp diffraction peaks at 20°~30° that belonged to the DHQ, disappeared. This indicates that DHQ and β-CD were transformed from a crystalline state to an amorphous state. The fact that the XRD patterns of DHQ and β-CD are completely different from those of the DHQ/β-CD complex suggests the possibility of inclusion complex formation.

^{1}H NMR analysis

^{1}H NMR spectra of β-CD and DHQ/β-CD complex are shown in Fig. 2D. The peak at 4.79 ppm was related to the protons of the D_2O solvent. It is known that β-CD molecule possesses the unique structure of a torus. In the ^{1}H NMR spectrum of β-CD, the H-1, H-2, H-4, and H-6 of β-CD were all located outside the cavity, while

Table 1 ^{1}H NMR (D_2O) chemical shift (δ) values of β-CD and DHQ/β-CD complex

Hydrogen atom	Splitting	δ (ppm)		$\Delta\delta_H$
		β-CD	DHQ/β-CD complex	
H-1	d	5.07	5.04	0.03
H-2	dd	3.65	3.64	0.01
H-3	dd	3.97	3.93	0.04
H-4	dd	3.59	3.58	0.02
H-5	m	3.87	3.80	0.07
H-6	dd	3.87	3.80	0.07

H-3 was located in medial to the wide ostial end, and H-5 was located in medial to the narrow ostial end (Silva et al. 2020).The chemical shifts of β-CD in the free and complex states are summarized in Table 1, and it can be seen that all β-CD protons are significantly shifted to the right to a certain content. The ΔδH of H-1, H-2, and H-4 were 0.03, 0.01, and 0.02 ppm, respectively. However, the chemical shift changes of H-3 and H-5 (0.04 and 0.07 ppm) were slightly larger than those of H-1, H-2, and H-4. Moreover, the change in chemical shift of H-5, located at medial and narrow ostial, is larger than that of H-3 located at the wide ostial end. This indicates that DHQ enters from the narrow ostial end of β-CD.

Molecular docking analysis

Molecular docking that based on the "lock and key" principle, was used to elucidate the binding mode and estimate the binding energy between DHQ and β-CD (Li et al. 2022). When DHQ is included, β-CD as the host molecule will change its shape to fit the binding and maximal the stabilization, and DHQ as the guest molecule will also adjust until the most stable supramolecular interactions are gained. The binding of β-CD and DHQ is not static or permanent but rather is a dynamic equilibrium. The molecular docking results revealed that DHQ could simply enter the cavity of β-CD stably and easily fits in the cavity, however its orientation in the cavity is variable. There were two main docking configurations for the β-CD/DHQ complex (Fig. 3B). One was where the A and B rings of DHQ were located at the wide and narrow ostial of β-CD, respectively, while the C ring of DHQ was inserted into the cavity. Relative vertical and lateral views was shown in Fig. 3C and E and the docking energy was − 5.56 kcal/mol.

The other one was where the A and B rings were located at the narrow and wide ostial end of β-CD, respectively, and the C ring of DHQ was also inserted into the cavity. Its vertical and lateral views were shown in Fig. 3D and F. The binding energy of β-CD with DHQ in this conformation was − 5.22 kcal/mol. In both conformations above, DHQ was theoretically well encapsulated with β-CD.

SEM analysis

SEM is a qualitative method to analyze the morphological aspects of the DHQ/β-CD complex. This technique, in conjunction with DSC and XRD, allows observing changes in the morphology of the DHQ/β-CD complex and provides indirect evidence of the presence of the new solid phase. As can be seen in Fig. 4, DHQ had an irregular acicular crystal shape, which is consistent with the previous report by Roman et al. (Terekhov et al. 2020). While β-CD showed irregular prismatic structure with a loose porous surface, which is also in agreement with a previous report (Gürten et al. 2018). The SEM image of DHQ/β-CD physical mixture showed it was a simple mixture of irregular acicular crystals of DHQ and irregular prismatic of β-CD. The DHQ/β-CD complex appeared to have a homogeneous blocky structure. Apparently, the morphology of the complex was significantly different from that of DHQ and β-CD.

Determination of particle size, solubility and dissolution rate

The particle size of the new substance was 0.70 ± 0.02 mm, which was 4.2 times that of pure DHQ 2.90 ± 0.03 mm. The solubility of DHQ at 25 ± 1 ℃ was 1.71 ± 0.16 mM, and the solubility of the prepared new substance was increased to 38.69 ± 1.45 mM. The solubility of the new substance in PBS was 25 °C, which was 22.63 times higher than that of pure DHQ.

The dissolution rate results of DHQ and new substance in PBS buffer were shown in Fig. 5. The cumulative dissolution of DHQ of the new substance over 60% in the first 5 min, and the dissolution plateaued at 97% after 160 min and remained stable. The accumulation of DHQ was only 16.03% in the first 5 min and rose to 60% after 40 min, after which remained stable. The product obtained from the lyophilized preparation consisted of the newly formed DHQ/β-CD inclusion complex and part of the amorphous DHQ. Their presence allows for increased solubility and dissolution. The increased solubility and dissolution rate of the new substance means that, after oral administration, more DHQ could be released from the new substance in the intestinal tract which will enhance the bio-accessibility and bioavailability of DHQ.

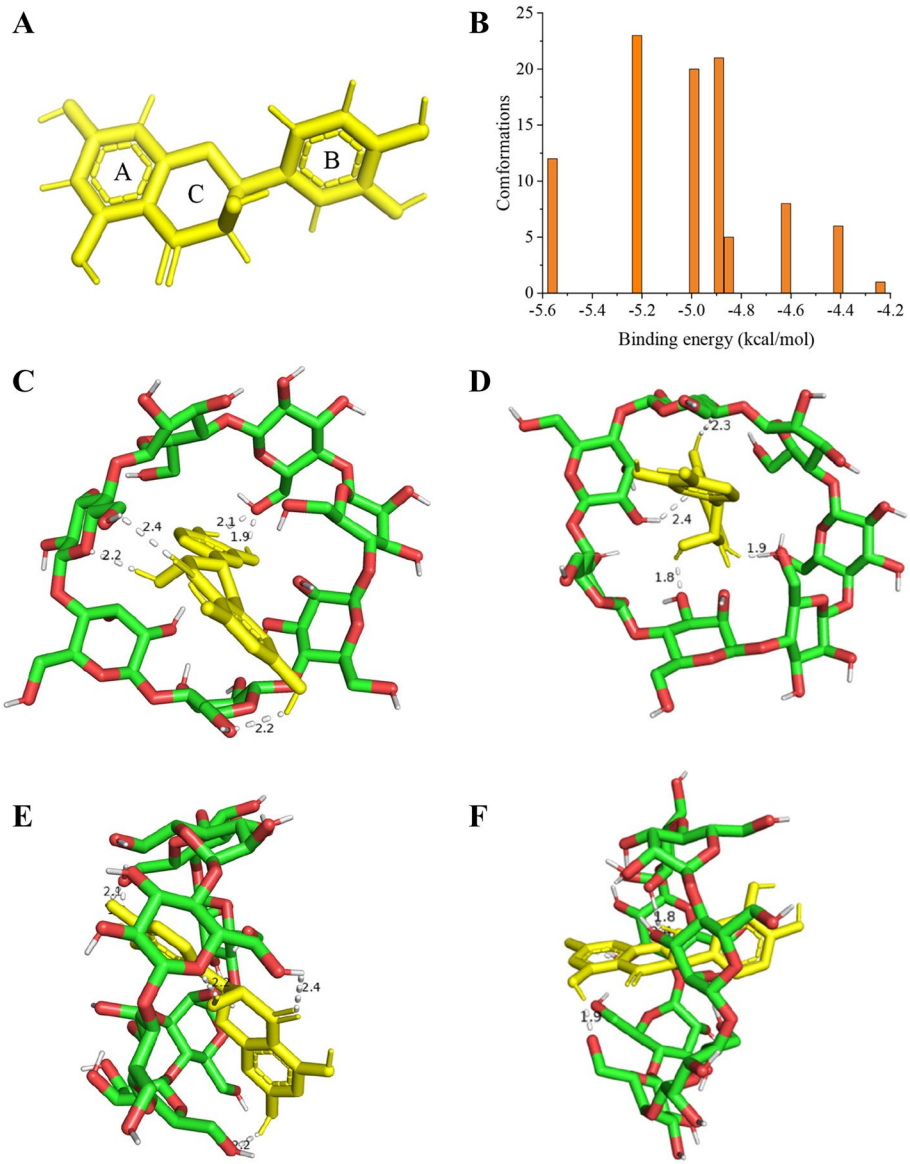

Fig. 3 Molecular docking analysis for the DHQ /β-CD complex. It was shown that DHQ could enter the cavity of β-CD and form stable complex. **A** is the structural formula for DHQ. **B** is a plot of the number of conformations versus the magnitude of the binding energy. **C** and **D** are the vertical views of the most stable docking conformations, and **E** and **F** are relative lateral views

TGA

The results on the thermal stability of DHQ,β-CD, DHQ/β-CD physical mixture and DHQ/β-CD complex are shown in Fig. 6. The thermogravimetric profile of DHQ was biphasic (Fig. 6A). In the first, slow phase, the weight of DHQ was initially reduced by 4.62% due to water loss in the temperature range of 30 ~ 250 °C. In the second, fast phase, the weight of DHQ decreased by 43.39% in the temperature range of 250 ~ 600 °C as a result of thermal decomposition. The thermogravimetric profile of the DHQ/β-CD complex was also biphasic (Fig. 6B). Compared to DHQ, the first, slow phase due to the water loss, covered a larger temperature range, namely from 30 °C to 280 °C, and the decrease was somewhat more, namely 9.55%. The second phase from 280 °C to 600 °C showed a weight decrease of 71.21%. That the second phase started at a higher temperature indicated that encapsulating of DHQ with β-CD makes DHQ, more stable, a phenomenon that is expected.

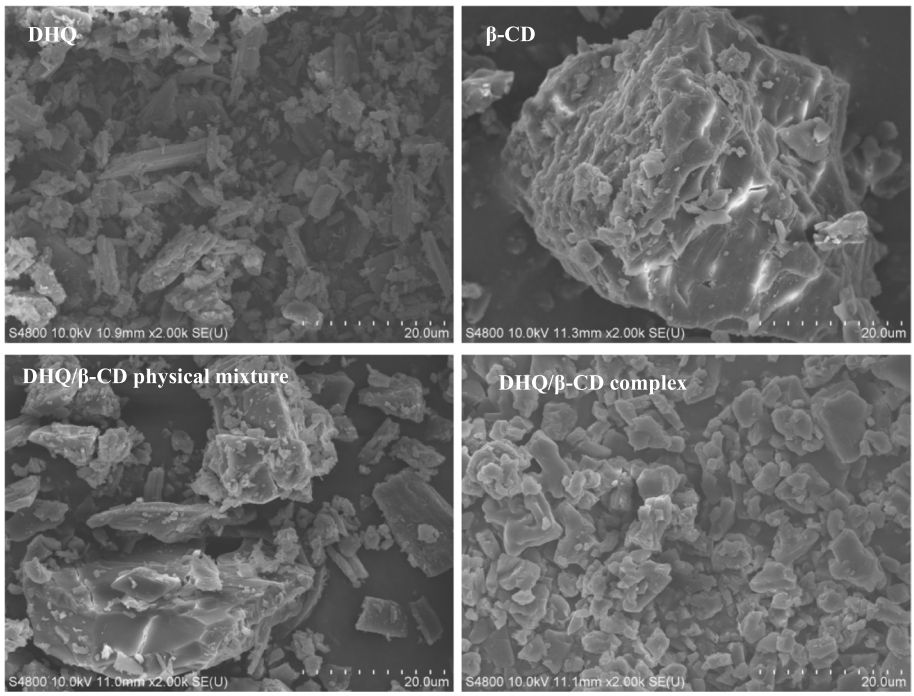

Fig. 4 SEM image of DHQ, β-CD, DHQ/β-CD physical mixture, and DHQ/β-CD complex

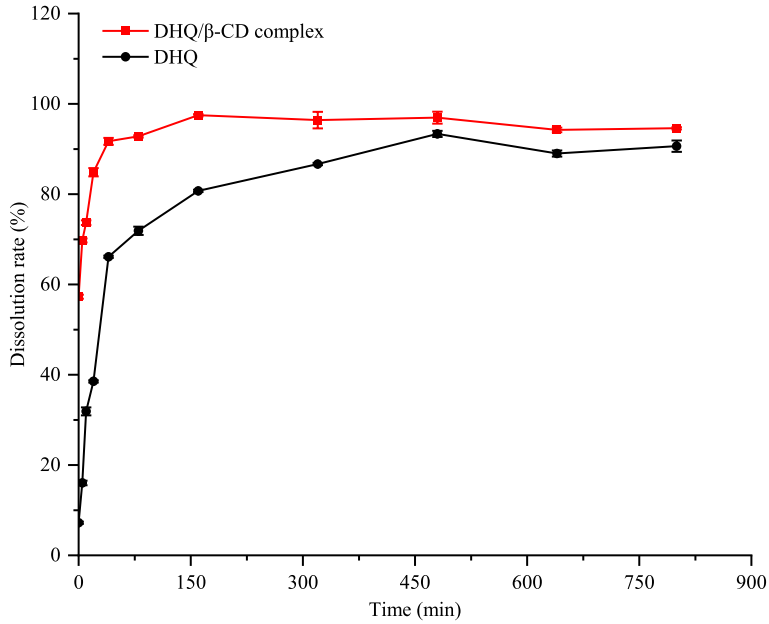

Fig. 5 Dissolution rate of DHQ/β-CD complex and DHQ in PBS buffer

However, a higher thermal stability was contradicted by the higher weight loss of the DHQ/β-CD complex in the second phase. The latter might be explained by the 4.2 times smaller particle size of the DHQ/β-CD complex compared with that of DHQ (Paola 2015). A greater surface area of the smaller DHQ/β-CD complex particles, makes it more prone to thermal decomposition.

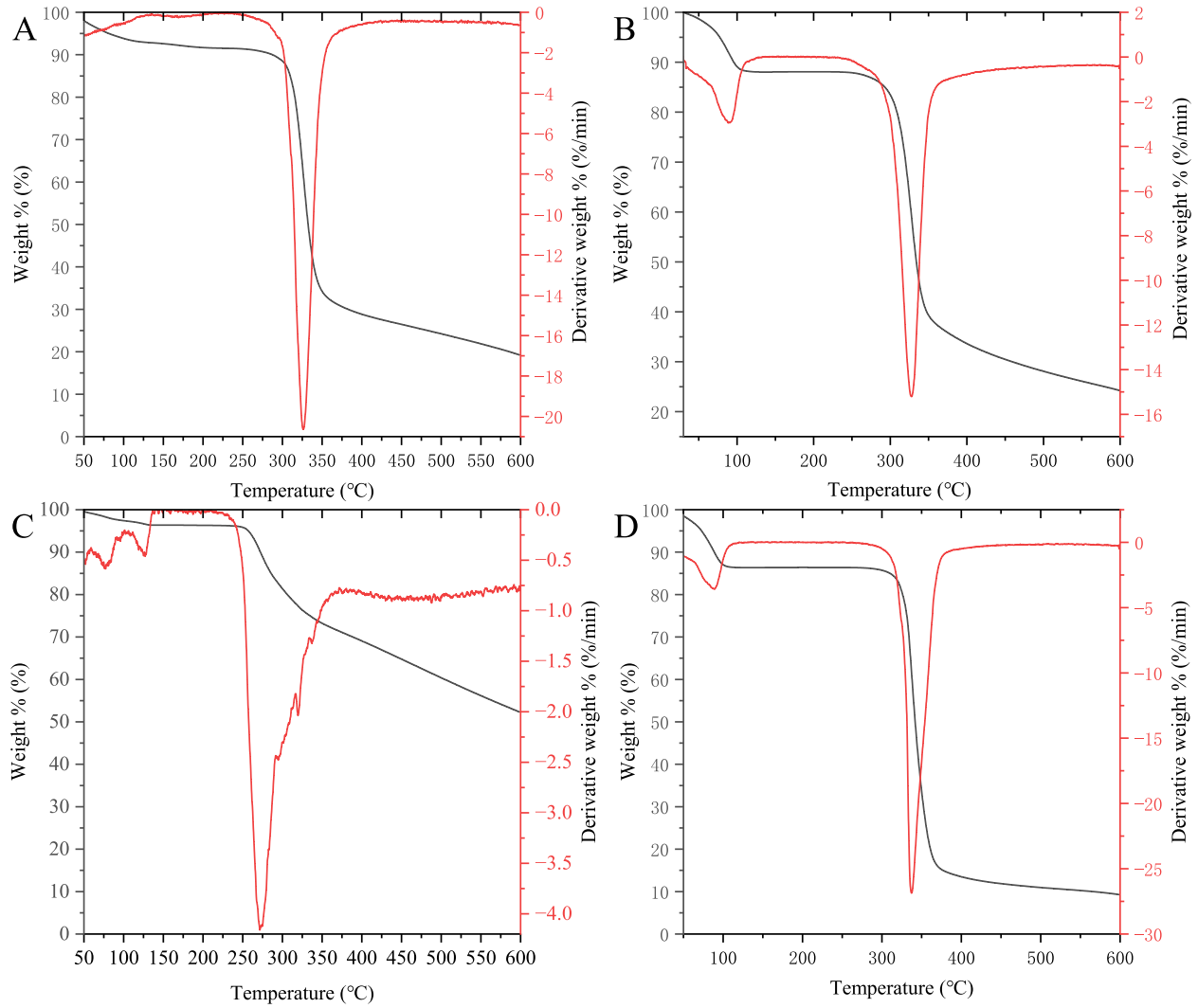

Fig. 6 Results of thermogravimetric analysis and derivative thermogravimetry of DHQ/β-CD complex (**A**), DHQ/β-CD physicial mixture (**B**), DHQ (**C**), and β-CD (**D**).The rate of the weight loss of DHQ was maximal at 271 ℃, while the DHQ/β-CD complex had this maximum at 327 ℃

Antioxidant activity analysis

The free radicals like hydroxyl, hydrogen peroxide, alkyl, sulfhydryl, phenoxy and p-phenylene, are proved to cause biological damage (Gebicki and Nauser 2021). The DPPH and ABTS radical scavenging activity are widely used to evaluate the of antioxidant ability of polyphenols like quercetin, epicatechin and rutin (Kim et al. 2022). CD cavity does not affect antioxidant capacity (Zuluaga et al. 2017). The free radical scavenging activity of DHQ and DHQ/β-CD complex of DPPH and ABTS radicals is shown in Fig. 7. It can be seen that the scavenging activity of DHQ/β-CD complex on DPPH and ABTS was both significantly higher than that of DHQ. The DPPH scavenging activity of DHQ/β-CD complex increased with the DHQ concentration (0.01 ~ 0.05 mM). When the DHQ concentration was 0.05 mM, the DPPH scavenging of DHQ and DHQ/β-CD complex increased to 54.01 ± 0.16% and 65.22 ± 0.08%, respectively. A similar result was also obtained in ABTS scavenging activity, in which the scavenging activity of DHQ and DHQ/β-CD complex reached 52.12 ± 1.94% and 64.96 ± 0.84%, respectively, when concentration of DHQ was increased to 0.01 mM. The results showed no free radical scavenging activity of β-CD and therefore data are not shown, which is consisted to published literature (Zuluaga et al. 2017). The results indicate that the antioxidant activity of DHQ is increased after being encapsulated by β-CD. This may be due to the improved DHQ stability after DHQ

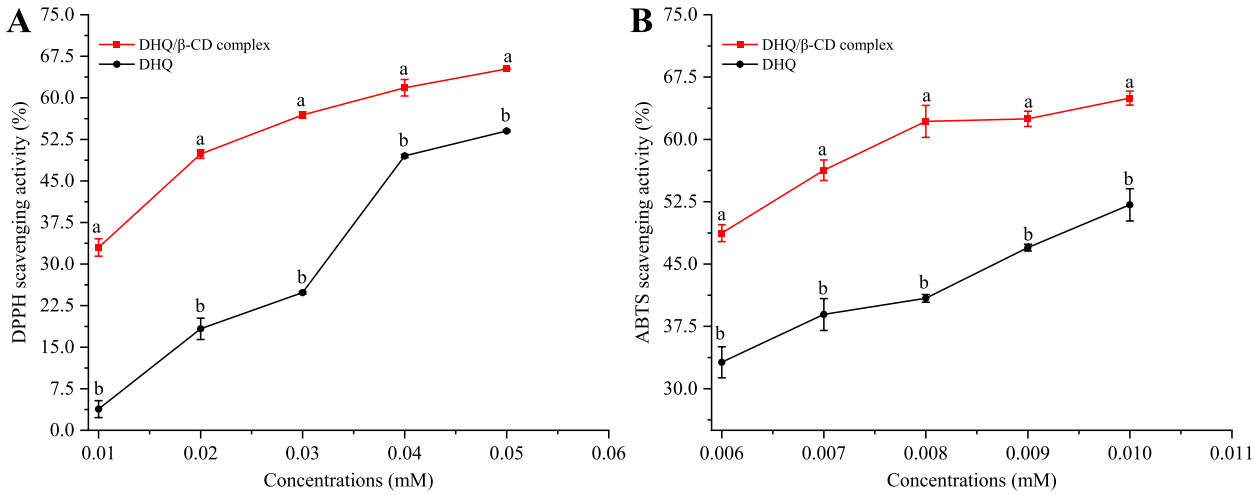

Fig. 7 Free radical scavenging activity of DHQ and DHQ/β-CD complex on DPPH (**A**) and ABTS (**B**) radicals

Table 2 The diameter of inhibition zone of DHQ, β-CD and DHQ/β-CD complex on *E. coli*

Concentration (mM)	Inhibition zone size (mm)				
	1.3	2.6	3.9	5.2	6.5
DHQ	8.42 ± 0.15[b]	8.97 ± 0.48[b]	9.56 ± 0.94[b]	10.7 ± 1.08[b]	11.64 ± 1.37[b]
DHQ/β-CD complex	9.07 ± 0.29[a]	11.02 ± 1.01[a]	11.72 ± 1.24[a]	12.2 ± 1.2[a]	13.66 ± 1.13[a]
β-CD	–	–	–	–	–
Control/sterile water	–	–	–	–	–

[a,b] Values in the same column with different letters are significantly different ($p < 0.05$)

is embedded into the β-CD cavity, making it easier to donate electrons to free radicals.

Antibacterial activity analysis

DHQ has an efficient antibacterial activity towards *Escherichia coli* (*E. coli)* (An et al. 2022). It is speculated that the hydrogen atom in the hydroxyl group on DHQ can interact with the phospholipid molecule in the cell membrane of *E. coli* via hydrogen bond, thus making the membrane structure loose (Kolhir et al. 1996). The inhibition effect of DHQ/β-CD complex on *E. coli* was studied, with sterile water, β-CD and DHQ as controls. As shown in Table 2, in the concentration range of DHQ from 1.3 to 6.5 mM, the antibacterial effect of the DHQ/β-CD complex on *E. coli* was significantly enhanced with the concentration increase of DHQ (1.3 ~ 6.5 mM). It was also shown that the antibacterial effect of DHQ/β-CD complex was significantly higher than that of DHQ. For example, at 6.5 mM, the diameter of the inhibition zone of DHQ was 11.64 ± 1.37 mm, which increased to 13.66 ± 1.13 mm for DHQ/β-CD complex. This is probably due to the higher solubility and dissolution rate of DHQ after encapsulating by β-CD.

Conclusions

A complex of DHQ with β-CD was successfully prepared by freeze drying at a 1:1-M ratio. The result of ^{1}H NMR and molecular docking showed that DHQ interacted with β-CD in the cavity via hydrogen bonds. The new substance composed of amorphous DHQ and DHQ/β-CD inclusion complex improved its solubility and dissolution rate compared with pure DHQ, the solubility of the DHQ was drastically increased (by 22.63-fold). The dissolution rate, the antioxidant activity and antibacterial activity of the DHQ were also significantly increased. Apparently, the preparation of DHQ/β-CD inclusion complex by freeze-drying method solves the problem of the poor aqueous solubility of DHQ, and broadens the path for a more optimal use of the health promoting effect of DHQ in pharmaceutical and food products.

Authors' contributions

Yaping Xu: writing original draft and editing. Yue Wang: investigation and software. Chujie Li: Validation. Tao Han: resources and software. Haiming Chen: methodology. Wenxue Chen: Data curation, resources. Qiuping Zhong: investigation. Jianfei Pei: methodology. Guido R.M.M. Haenen: Review and editing. Zhengwen Li: methodology and software. Mohamed Moalin: review

and editing. Ming Zhang: writing, reviewing and editing. Weijun Chen: methodology and funding acquisition. All authors read and approved the final manuscript.

Declarations

Availability of data and materials
The datasets used and/or analyzed the current study are available from the corresponding author on reasonable request.

Competing interests
The authors declare that they have no competing interests.

Funding
This work was financially supported by Hainan Provincial Natural Science Foundation of China (221QN174), the National Natural Science Foundation of China (32201977), and the Scientific Research Foundation of Hainan University (KYQD (ZR)-21045).

Acknowledgements
The author would like to thank the people of the Fruit and Vegetable Processing Team at the School of Food Science and Engineering of Hainan University.

Authors' information
Not applicable.

Received: 14 March 2023 Accepted: 29 August 2023
Published online: 03 October 2023

References

An H, Yoon Y, Lee J, Jeong N (2022) Antioxidant and antimicrobial properties of dihydroquercetin esters. Braz J Pharm Sci 58:e190800
Benguo L, Wei L, Jian Z, Yang L, Xiaoai Z, Guizhao L (2013) Physicochemical characterisation of the supramolecular structure of luteolin/cyclodextrin inclusion complex. Food Chem 141(2):900–906
Brewster ME, Loftsson T (2007) Cyclodextrins as Pharmaceutical Solubilizers Adv Drug Deliver Rev 59(7):645–666
Cao H, Chen X, Yamamoto K (2012) Bovine serum albumin significantly improves the DPPH free radical scavenging potential of dietary polyphenols and gallic acids. Anti-Cancer Agent ME 12(8):940–948
Carlotti ME, Sapino S, Ugazio E, Caron G (2011) On the complexation of quercetin with methyl-β-cyclodextrin: photostability and antioxidant studies. Jincl Phenom Macro 70(1–2):81–90
Cenobio-Galindo ADJ, Ocampo-López J, Reyes-Munguía A, Carrillo-Inungaray ML, Cawood M, Medina-Pérez G, Fernández-Luqueño F et al (2019) Influence of bioactive compounds incorporated in a nanoemulsion as coating on avocado fruits (persea americana) during postharvest storage: antioxidant activity, physicochemical changes and structural evaluation. Antioxidants 8(10):500
Conceicao J, Adeoye O, Cabral-Marques HM, Lobo JMS (2018) Cyclodextrins as drug carriers in pharmaceutical technology: the state of the art. Curr Pharm Design 13(24):1405–1433
Crini G (2014) Review: a history of cyclodextrins. Chem Rev 21(114):10940–10975
Farahat MG (2020) Enhancement of β-cyclodextrin production and fabrication of edible antimicrobial films incorporated with clove essential oil/β-cyclodextrin inclusion complex. Microbiol Biotechnol Lett 48(1):12–23
Gebicki JM, Nauser T (2021) Fast antioxidant reaction of polyphenols and their metabolites. Antioxidants 10(8):1297
Guedes L, Morgon N, Martins M, Pessine F (2020) Imiquimod/β-Cyclodextrin inclusion complex: experimental and theoretical studies. J Brazil Chem Soc 31(8):1732–1745
Gürten B, Yenigül E, Sezer AD, Malta S (2018) Complexation and enhancement of temozolomide solubility with cyclodextrins. Braz J Pharm Sci 54(2):e17513
He R, Zhang Z, Xu L, Chen W, Zhang M, Zhong Q et al (2022) Antibacterial mechanism of linalool emulsion against pseudomonas aeruginosa and its application to cold fresh beef. World J Microbiol Biotechnol 4(38):56
Huo D, Liu X, Zhang Y, Duan J, Zhang Y, Luo J (2020) A Novel R2R3-MYB transcription factor PqMYB4 inhibited anthocyanin biosynthesis in Paeonia qiui. Int J Mol Sci 21(16):5878
Katanic J, Boroja T, Stankovic N, Mihailovic V, Mladenovic M, Kreft S et al (2015) Bioactivity, stability and phenolic characterization of Filipendula ulmaria (L.) Maxim. Food Funct 6(4):1164–75
Khanna S, Chakraborty J (2018) Mosquito repellent activity of cotton functionalized with inclusion complexes of β - cyclodextrin citrate and essential oils. Fash Text. 5(9).
Khlupova M, Vasil Eva I, Shumakovich G, Morozova O, Chertkov V, Shestakova A et al (2016) Laccase-mediated biotransformation of dihydroquercetin (taxifolin). J Mol Catal B Enzym 123:62–66
Kim J (2020) Synthesis and characterization of phenolic acid/hydroxypropyl-beta-cyclodextrin inclusion complexes. Prev Nutr Food Sci 25(4):440–448
Kim S, Yoo N, Choi S (2022) Interactions between ZnO nanoparticles and polyphenols affect biological responses. Nanomaterials 12(19):3337
Kolhir VK, Bykov VA, Baginskaja AI, Sokolov SY, Glazova NG, Leskova TE et al (1996) Antioxidant activity of a dihydroquercetin isolated from larix gmelinii (Rupr.) Rupr. Wood Phytother Res 10(6):478–82
Kurth EF, Frank LC (1951) Dihydroquercetin as an antioxidant. J Am Oil Chem Soc 28(10):433–436
Li T, Guo R, Zong Q, Ling G (2022) Application of molecular docking in elaborating molecular mechanisms and interactions of supramolecular cyclodextrin. Carbohyd Polym 276:118644
Lia JX, Dong JQ, Ouyang J, Cui J, Chen Y, Wang FJ et al (2016) Synthesis, characterization, solubilization, cytotoxicity and antioxidant activity of aminomethylated dihydroquercetin. Medchemcomm 8(2):353–363
Liu Y, Chen Y, Gao X, Fu J, Hu L (2020) Application of cyclodextrin in food industry. Crit Rev Food Sci 62(10):2627–2640
Liu N, Chen H, Yang Z, Xia M, Wang D, Zang L et al (2022) Enhancement of dissolving capacity and reducing gastric mucosa irritation by complex formation of resibufogenin with β-Cyclodextrin or 2-Hydroxypropyl-β-cyclodextrin. Molecules 27(10):3213
Paola M (2015) Analytical techniques for characterization of cyclodextrin complexes in the solid state: a review. J Pharmaceut Biomed 113:226–238
Priya D, Meenakshi B (2020) Pharmaceutical applications of cyclodextrins and their derivatives. J Incl Phenom Macro 98(3–4):171–186
Qi QS, Zimmermann W (2005) Cyclodextrin glucanotransferase: from gene to applications. Appl Microbiol Biot 66(5):475–485
Qian L, Hongyu P, Peixiao T, Bin T, Qiaomei S, Hui L (2018) Propyl gallate/cyclodextrin supramolecular complexes with enhanced solubility and radical scavenging capacity. Food Chem 245:1062–1069
Sadaquat H, Akhtar M (2020) Comparative effects of β-cyclodextrin, HP-β-cyclodextrin and SBE7-β-cyclodextrin on the solubility and dissolution of docetaxel via inclusion complexation. J Incl Phenom Macro 96(3–4):333–351
Savic IM, Nikolic VD, Savic-Gajic I, Nikolic LB, Radovanovic BC, Mladenovic JD (2015) Investigation of properties and structural characterization of the quercetin inclusion complex with (2-hydroxypropyl)-β-cyclodextrin. J Incl Phenom Macro 82(3–4):383–394
Selivanova IA, Terekhov RP (2020) Engineering of dihydroquercetin crystals. Pharm Chem J 53(11):53–57
Shanmugam A, Kathiresan K, Nayak L (2016) Preparation, characterization and antibacterial activity of chitosan and phosphorylated chitosan from cuttlebone of Sepia kobiensis (Hoyle, 1885). Biotechnol Rep 9:25–30
Silva I, Feitosa E, Santos M, Silva R, Rocha M, Da Silva F et al (2020) Theoretical and experimental investigations on inclusion complex β-Cyclodextrin and sulcatone: a cardiovascular activity evaluation. J Brazil Chem Soc 31(5):1064–1077
Song L, William CP (1992) Cyciodextrins and their applications in analytical chemistry. Chem Rev 92:1457–1470
Terekhov RP, Selivanova IA, Tyukavkina NA, Ilyasov IR, Zhevlakova AK, Dzuban AV et al (2020) Assembling the puzzle of taxifolin polymorphism. Molecules 25(22):5437
Viswalingam M, Prabu S, Sivakumar K, Rajamohan R (2016) Preparation and characterization of a imipramine-ß-cyclodextrin inclusion complex. Instrum Sci Technol 44(6):651–671

Wan J, Long Y, Zhang Y, Xiang Y, Liu S, Li N et al (2021) A novel technology to reduce astringency of tea polyphenols extract and its mechanism. Chin Herb Med 13(3):421–429
Wang T, Li B, Feng Y, Guo Q (2011) Preparation, quantitive analysis and bacteriostasis of solid state iodine inclusion complex with β-cyclodextrin. Jincl Phenom Macro 69(1–2):255–262
Wen L, Jiang Y, Yang J, Zhao Y, Tian M, Yang B (2017) Structure, bioactivity, and synthesis of methylated flavonoids. Ann Ny Acad Sci 1398(1):120–129
Yan Z, Juan Y, Xiao-Dan D, Hai-Yu J (2017) Research on characteristics, antioxidant and antitumor activities of dihydroquercetin and its complexes. Molecules 23(1):20
Yang LJ, Chen W, Ma SX, Gao YT, Huang R, Yan SJ et al (2011) Host–guest system of taxifolin and native cyclodextrin or its derivative: preparation, characterization, inclusion mode, and solubilization. Carbohydr Polym 85(3):629–637
Yuangang Z, Weiwei W, Xiuhua Z, Yong L, Weiguo W, Chen Z et al (2014) Enhancement of solubility, antioxidant ability and bioavailability of taxifolin nanoparticles by liquid antisolvent precipitation technique. Int J Pharmaceut 471(1–2):366–376
Zhang X, Ruan Y, Liu W, Chen Q, Gu L, Guo A (2020) Transcriptome analysis of gene expression in dermacoccus abyssi HZAU 226 under lysozyme stress. Microorganisms 8(5):707
Zhou W, Lv XF, Hei MR, Zhao YY, Cui ZK, Zhang H (2022) Preparation and characterization of an oridonin and γ-cyclodextrin complex. Food Sci Tech-Brazil 42:e68722
Zu Y, Wu W, Zhao X, Li Y, Zhong C, Zhang Y (2014) The high water solubility of inclusion complex of taxifolin-γ-CD prepared and characterized by the emulsion solvent evaporation and the freeze drying combination method. Int J Pharm 477:148–158
Zuluaga M, Barzegari A, Letourneur D, Gueguen V, Pavon-Djavid G (2017) Oxidative stress regulation on endothelial cells by hydrophilic astaxanthin complex: chemical, biological, and molecular antioxidant activity evaluation. Oxid Med Cell Longev 2017:1–15

Publisher's Note